



Aromatic stacking - the key step in the nucleation of aromatic benzoic acids

DOI:

[10.1039/C7CC02423A](https://doi.org/10.1039/C7CC02423A)

Document Version

Accepted author manuscript

[Link to publication record in Manchester Research Explorer](#)

Citation for published version (APA):

Cruz Cabeza, A., Davey, R., Salim Sachithanathan, S., Smith, R., Tang, S. K., Vetter, T., & Yang, X. (2017). Aromatic stacking - the key step in the nucleation of aromatic benzoic acids. *Chemical Communications*. <https://doi.org/10.1039/C7CC02423A>

Published in:

Chemical Communications

Citing this paper

Please note that where the full-text provided on Manchester Research Explorer is the Author Accepted Manuscript or Proof version this may differ from the final Published version. If citing, it is advised that you check and use the publisher's definitive version.

General rights

Copyright and moral rights for the publications made accessible in the Research Explorer are retained by the authors and/or other copyright owners and it is a condition of accessing publications that users recognise and abide by the legal requirements associated with these rights.

Takedown policy

If you believe that this document breaches copyright please refer to the University of Manchester's Takedown Procedures [<http://man.ac.uk/04Y6Bo>] or contact uml.scholarlycommunications@manchester.ac.uk providing relevant details, so we can investigate your claim.



ChemComm

Accepted Manuscript



This article can be cited before page numbers have been issued, to do this please use: A. Cruz-Cabeza, R. J. Davey, S. Salimsachithanantha, R. Smith, S. K. Tang, T. Vetter and Y. Xiao, *Chem. Commun.*, 2017, DOI: 10.1039/C7CC02423A.



This is an Accepted Manuscript, which has been through the Royal Society of Chemistry peer review process and has been accepted for publication.

Accepted Manuscripts are published online shortly after acceptance, before technical editing, formatting and proof reading. Using this free service, authors can make their results available to the community, in citable form, before we publish the edited article. We will replace this Accepted Manuscript with the edited and formatted Advance Article as soon as it is available.

You can find more information about Accepted Manuscripts in the [author guidelines](#).

Please note that technical editing may introduce minor changes to the text and/or graphics, which may alter content. The journal's standard [Terms & Conditions](#) and the ethical guidelines, outlined in our [author and reviewer resource centre](#), still apply. In no event shall the Royal Society of Chemistry be held responsible for any errors or omissions in this Accepted Manuscript or any consequences arising from the use of any information it contains.



Chemical Communications

COMMUNICATION

Aromatic stacking – a key step in nucleation[†]Aurora J. Cruz-Cabeza,^{[a]*} Roger J. Davey,^{[a]*} Sharlinda Salim Sachitananthan,^[a] Rebecca Smith,^[a] Sin Kim Tang,^[a] Thomas Vetter^[a] and Yan Xiao^[b]Received 00th January 20xx,
Accepted 00th January 20xx

DOI: 10.1039/x0xx00000x

www.rsc.org/

Crystal nucleation from solution is of central importance in the chemical and biological sciences. Linking nucleation kinetics to the properties of solutes and solvents remains a grand-challenge in physical chemistry. Through a unique dataset of compounds able to self-assemble via both hydrogen-bonds and aromatic stacking, we are able to compare the importance of these two types of interaction in driving the nucleation process. Contrary to previous reports in which solution chemistry and hydrogen bonding have been seen as controlling factors, we are now able to show that cluster growth via aromatic stacking holds the key.

There can be no question of the central importance that crystal nucleation^[1] plays across not only the physical and biological sciences but also in the industrial context of materials chemistry. For example, *in-vivo* crystal nucleation of β -hematin is known to be a key process for the survival of the malaria parasite.^[2] Indeed the biological activity of some antimalarial drugs is believed to result from their interference with this process. In the worlds of biomineralisation and protein crystallisation the discovery of solution mediated pre-nucleation clusters and liquid-like phases have been seen as major advances in understanding, for example, the nucleation of calcium carbonate^[3] and of lysozyme.^[4] In the pharmaceutical sciences (which supports a market of ca. a trillion US\$ and isolates 90% of its products as crystalline molecular solids) the control of nucleation is essential for the processing and formulation of active ingredients into medicines.^[5] Understanding the key intermolecular interactions and molecular processes which underpin nucleation is, therefore, essential and yet despite the existence of sophisticated theoretical treatments^[1a] much remains to be done.

In recent years a resurgence of interest in this topic has taken place, particularly for the nucleation of molecular crystals from

solution^[6]. This has been driven by a number of key developments: increasing computational power enabling the study of larger ensembles of molecules,^[7] the availability of medium throughput reactor devices for performing multiple experimental repeats and, vitally, a range of accessible *in situ* microscopic and spectroscopic techniques.^[8]

A molecular understanding of processes occurring during the early stages of crystal formation has been largely overlooked^[9a,b] and is predicated on the interpretation of reliably measured nucleation kinetics. Such data can be accumulated via medium throughput methods as in the Crystal16 methodology of Jiang and ter Horst^[10] for the evaluation of nucleation rates from induction time measurements. This, and other^[11] techniques have enabled an increasing availability of kinetic data relating nucleation rates to supersaturation and solvent choice. However, up until now the systems studied appear to have been chosen at random.^[9a,12] If we are to further our understanding of the relationship between molecular structure, crystal structure, solution chemistry and nucleation kinetics then study of a series of structurally related molecules is essential.^[13] Accordingly, we report on a group of four related benzoic acids (Fig.1) nucleating from acetonitrile (MeCN), toluene, ethyl acetate (EA) and isopropanol (IPA) (*nb* for solubility reasons IPA/water 1:2 mixture was used for benzoic acid). Our overall objective was to obtain mechanistic insights through correlations of the measured relative nucleation kinetics (as functions of solvent and solute) with thermodynamic, structural and molecular-scale properties of the acids.

These four molecules provide an attractive group since not only do they all contain the important carboxylic acid functionality but

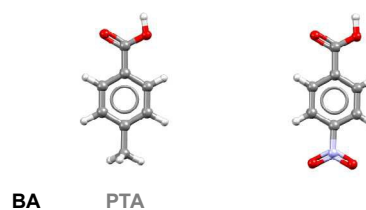


Figure 1. Molecular structures of benzoic acid (BA), p-toluic acid (PTA), p-aminobenzoic acid (PABA) and p-nitrobenzoic acid (PNBA).

^a School of Chemical Engineering and Analytical Science, University of Manchester, Manchester, United Kingdom.

^b State Key Laboratory of Chemical Engineering, School of Chemical Engineering and Technology, Tianjin University, Tianjin, P.R. China

Corresponding authors:
aurora.cruzcabaza@manchester.ac.uk
roger.davey@manchester.ac.uk

[†] Authors are listed alphabetically; their contributions are detailed in ESI. Electronic Supplementary Information (ESI) available: experimental and computational procedures; further correlations. See DOI: 10.1039/x0xx00000x

COMMUNICATION

Chemical Communications

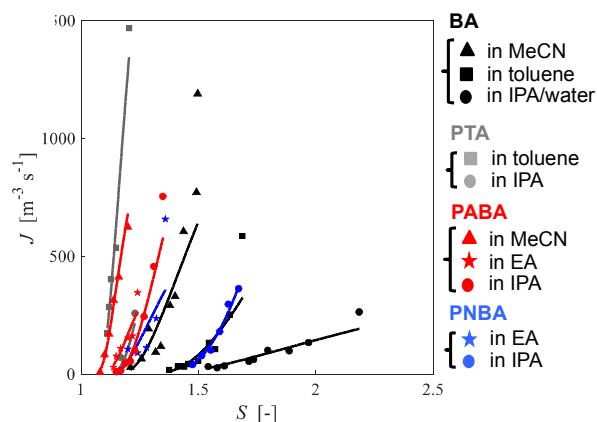


Figure 2. Nucleation rates (J) as a function of supersaturation (S) for BA, PTA, PNBA and PABA in various solvents. Lines are derived by fitting the data to the classical nucleation theory interface transfer control nucleation equation (Eq. 1).

they also form crystal structures in which combinations of H-bonding and aromatic stacking determine the key packing motifs. This offered the prospect of identifying which assembly mode controls the nucleation process.

We derived crystal nucleation rates from induction time measurements for our four target compounds in various solvents and at different supersaturations using the Crystal16 methodology. All crystallisation experiments were performed by crash cooling to 20°C except for PNBA (25°C). Further details of the experimental procedure are given in the ESI, are well-documented in the literature^[10,12c,12e] and we have recently reported on the quantification of their uncertainties.^[20] These experimental nucleation rates (J) are plotted against solution supersaturations (S) in Figure 2. The generation of these data required over six thousand independent crystallisation experiments^[14] involving our four targeted acids, the four selected solvents and a range of supersaturations per system. Figure 2 allows us to derive a qualitative order of nucleation kinetics for our compounds and also for the various solvents independently. Firstly, if we consider each solute in turn it is roughly the case that the order of rates, from slowest to fastest, is BA < PNBA < PABA < PTA. Secondly, in terms of the solvent dependence it is evident that (for each solute) nucleation is always slowest from IPA solutions and fastest from MeCN.^[15] The solvent dependence of nucleation has been reported previously for datasets comprising single carboxylic acids (e.g. salicylic acid,^[12a] PABA^[9a]). In these studies, the relative difficulty of nucleation was correlated with the strength of solvation of the carboxylic acid group in each particular solvent and the associated difficulty of creating hydrogen-bonded dimers. Similar solvent correlations also appear to be true for our compounds if analysed individually across the range of solvents (i.e. strong solvation appears to slow down nucleation). However, when all the solute and solvent systems are taken together such a correlation breaks down. For example, the nucleation rates of BA and PTA differ by up to three orders of magnitude while neither the energies of their H-bonded dimers nor the strength of solvent binding to their acid groups can be expected to differ significantly in any solvent. PABA and PNBA have Hammett constants of -0.66

Table 1. Summary of the CNT thermodynamic and kinetic parameters derived from the nucleation rate measurements. 95% confidence intervals are given in parenthesis.

Solute	Solvent	$A \times 10^{12}$ ($\text{m}^{-3} \text{s}^{-1}$)	$B \times 10$	$f_0 C_0 / M$ ($\text{mol}^{-1} \text{s}^{-1}$) ^[a]	γ (mJ m^{-2})
BA	Toluene	13 (8.7-18)	5.2 (4.6-5.8)	10.0 (6.5-15.0)	4.4 (4.2-4.6)
	MeCN	11 (8.6-15)	1.6 (1.4-1.8)	4.5 (3.2-6.3)	3.0 (2.8-3.1)
BA	IPAW	1.8 (1.3-2.6)	4.5 (3.6-5.4)	1.4 (0.9-2.1)	4.2 (3.9-4.5)
PTA	Toluene	28 (16-47)	0.32 (0.23-0.40)	38 (19-73)	1.4 (1.3-1.5)
	IPA	21 (9-49)	1.1 (0.8-1.3)	8.2 (3-22)	8.2 (1.9-2.2)
PABA	MeCN	13 (9.2-18)	0.28 (0.23-0.32)	4.1 (2.7-6.2)	1.6 (1.5-1.7)
	EA	6.2 (3.8-9.8)	0.5 (0.37-0.62)	1.8 (0.97-3.2)	1.9 (1.7-2.1)
PABA	IPA	16 (11-23)	1.2 (1.0-1.3)	10.0 (6.8-15.0)	2.6 (2.5-2.7)
	IPA	37 (16-80)	7.4 (5.9-8.9)	201 (80-478)	4.6 (4.3-4.9)
PNBA	IPA	6.7 (4.6-9.6)	0.89 (0.72-1.1)	13 (8.3-21.0)	2.3 (2.1-2.4)
	EA	6.7 (4.6-9.6)	0.89 (0.72-1.1)	13 (8.3-21.0)	2.3 (2.1-2.4)

[a] $f_0 C_0$ is normalized by the solubility in mol m^{-3} .

and +0.78 respectively,^[16] meaning that the H-bonding of the acid group to a solvent would be stronger for PABA than for PNBA which in turn would imply that nucleation of PABA should be the slower if desolvation of the carboxylic acid alone was rate limiting. This is not the case, as shown by the data in Figure 2. Similar conclusions can be reached by examination of the FTIR carbonyl stretch region (~1700 cm^{-1}) of solutions of these acids.^[17] Identical solvation behaviour of BA and PTA in toluene and acetonitrile is confirmed by FTIR, highlighting again that carbonyl solvation cannot trigger the kinetic differences seen here.^[18]

Further analysis of the nucleation kinetics of our solutes was achieved by deriving a series of characteristic quantities from the nucleation rate data. Firstly, we used the measured values of J to estimate the supersaturation S_{200} at which for each solute/solvent system the nucleation rate achieves a value of $200 \text{ m}^{-3} \text{ s}^{-1}$ (ESI). This choice is made on the basis that for all the acids chosen S_{200} lies within the measured range (Fig. 2). Secondly, using Classical Nucleation Theory (CNT), eq. (1), (for interface-transfer-control) we derived the kinetic and thermodynamic parameters A and B for the four compounds in the various solvents (Table 1).^[19]

$$J = A S \exp\left(-\frac{B}{\ln^2 S}\right) \quad (1)$$

These parameters reflect the two processes that define a nucleation pathway, namely the number and size of the critical nuclei (related to B) and the growth of these nuclei through the critical size (related to A). Thus, from A we derived $f_0 C_0$ where f_0 is the supersaturation independent part of the molecular attachment frequency and C_0 is the concentration of nucleation sites.^[10b] From the thermodynamic parameter B , the interfacial energy γ of the cluster/solution interface was calculated. Values of these parameters are summarised in Table 1 for the various solute-solvent systems together with their 95% confidence intervals derived using the method of Xiao et al.^[20]

In attempting to use these data to reveal potential mechanistic processes underpinning nucleation we explored correlations with a number of intensive properties of the solute/solvent systems used. Experimentally derived

nucleation parameters showed *no* correlations with solute/solvent properties such as solubility, enthalpy of solution, or solvent dielectric constants (ESI). To go beyond such general considerations we then proceeded to compute lattice energies, solvation energies, crystallisation energies (the difference between the monomer energy in the crystal lattice and the energy of a monomer in solution), attachment energies and relative growth rates (G_{rel})^[21] for the four solutes in the various solvent environments. All energy calculations were done using DFT methods (PBE functional) with van der Waals corrections^[22] as implemented in the planewave-code VASP^[23] with the inclusion of implicit solvation models (VASP-sol).^[24] Further simulation details are given in the ESI. Relative growth rates were derived from computed attachment energies and crystal growth morphologies.

No significant correlations were found (see ESI) except for that seen in Figure 3 between the experimentally derived S_{200} and the computed relative crystal growth rates. We note two outliers (red points) corresponding to crystallisation experiments from acetonitrile, a feature we are currently investigating further. Overall, we observe that the higher the computed relative growth rates the lower the supersaturation values required to achieve the same nucleation rate of $200 \text{ m}^{-3} \text{ s}^{-1}$. Such a trend suggests that in the overall nucleation pathway from molecule to supramolecular cluster it is cluster growth through the critical size that is rate determining for these solutes. Indeed, this conclusion is supported by experimental growth rate data from macroscopic PABA^[5b] and BA^[5c] crystals where the relative rates follow an identical pattern.

Given that these cluster growth rates are calculated from attachment energies (which account for the many interactions in the crystal) we then attempted to discern a specific rate limiting molecular pathway by considering the strength of individual solvent dependent solute–solute interactions which must form as molecular attachment and consequent cluster growth proceed. To achieve this we assume firstly that clusters have the same packing as mature crystals and secondly that cluster growth occurs via desolvation and attachment of solution phase monomers to lattice sites on the cluster surface²⁵. In the crystal structures of these four acids two major solute–solute interactions were identified for consideration as the main contributors to molecular attachment - hydrogen-bonding and aromatic stacking. While the former leads to identical H-bonded dimers in each structure (Fig. 4a), the effect of different *para* substituents on molecular shape yields aromatic stacking motifs with considerably different geometric arrangements and ring overlaps (Fig. 4b; Table S8). To estimate the relative importance of these interactions as contributors to cluster growth, pairs of molecules (see Fig.4) related by H-bonding and aromatic stacking, were extracted from their crystal structures. For each acid the solvent dependent interaction energies were then calculated as the difference (in a given solvent) between two monomers and the extracted molecular pair (ESI). Thus, H-bonded dimerisation energies were computed to be virtually identical for each solute but dependent on the solvent environment^[26] (e.g. -89 kJ/mol in the gas-phase and -53 kJ/mol in MeCN, ESI). These data reconfirm the above assertion that desolvation of the carboxylic acid group cannot be the rate-limiting step. Aromatic stacking

energies of these solutes in the various solvents,

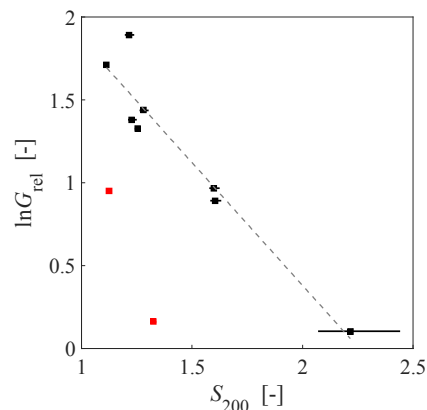


Figure 3. Correlation between S_{200} and the computed relative growth rates. Crystallisations from MeCN are depicted in red.

however, were found to differ considerably and Figure 5 shows the relation between stacking energies and the experimental S_{200} . The steady increase in S_{200} as the solvent dependent stacking energy decreases suggests that cluster growth is controlled by the attachment of molecules to growing aromatic stacks in the molecular clusters.

This finding is revealing since although aromatic stacking is a relatively weak interaction (between -10 and -30 kJ/mol), within the crystal structures of our four acids, stacking is the only continuous interaction propagating throughout the entire crystal and hence a crucial contributor to crystal growth. Thus from this foregoing analysis we have arrived at three major and important conclusions for our aromatic carboxylic acids: (i) the relative nucleation rates are not governed by monomer desolvation alone, (ii) the relative nucleation rates are intrinsically related to their solvent-dependent relative crystal growth rates and (iii) the relative nucleation rates are related to the solvent-dependent strength of aromatic stacking interactions. Thus we arrive at the view that the nucleation rate is determined by the rate of cluster growth which in turn is controlled by the attachment of molecules to the nucleus via aromatic stacking. The energetics of this process is solvent and solute dependent.

To our knowledge this is the first experimental study to link nucleation kinetics, solvent and molecular attachment across such a broad dataset and certainly the first to show the key role played by stacking interactions in the nucleation of aromatic carboxylic acids. These conclusions have important wider implications.

Firstly, while the self-assembly modes and consequent structure of clusters cannot be inferred from CNT, the success of our computational analysis rests on the assumption that clusters have the same packing as mature crystals^[8]. Given the size of the critical nucleus, as computed from the CNT values of B, Table 1, to be between 20 and 100 molecules^[9a] this is not unreasonable. Indeed it is completely consistent with the enormous body of existing work in which nucleation has been studied from a structural perspective [6].

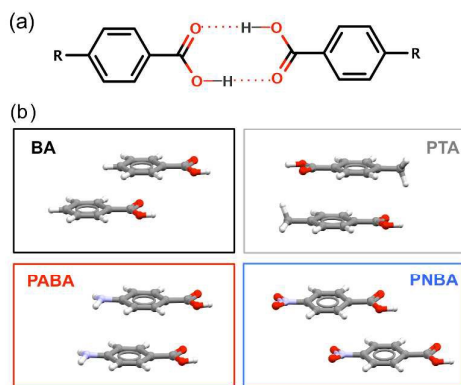


Figure 4. Geometries of solute-solute pairs, as present in the respective crystal structures of the model compounds, interacting via (a) hydrogen-bonding and (b) aromatic stacking.

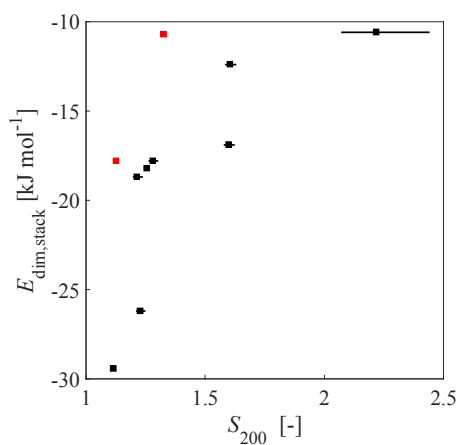


Figure 5. Correlation between S_{200} and the computed dimerisation energies for aromatic stacks. Crystallisations from MeCN are depicted in red.

There is thus no reason to invoke the idea of any form of disordered, precursor phase – based on our conclusions we may speculate that the origin of the clusters lies essentially in the formation of aromatic stacking interactions in solution. Indeed this suggestion appears to be consistent with recent reports on the solvent induced aggregation of *m*-aminobenzoic acid^[27] and imidazole^[28] for which stacking interactions play a central role. Secondly, we can make an important link between these kinetic data and the world of crystal structure prediction. Routine computation of solvent dependent relative growth rates as well as the energetics of propagating molecule-molecule interactions within a predicted set of structures would allow an experimental protocol to be devised aimed at selecting solvents offering the highest chance of nucleating desired computed structures.

Acknowledgements

YX, SSS and SKT gratefully acknowledge funding from the Chinese Scholarship Council, Majlis Amanah Rakyat Malaysia and Pfizer UK Ltd., respectively. RJD acknowledges helpful discussions with Prof. S. Schroeder, University of Leeds.

Notes and references

- a) D. Kashchiev, *Nucleation: Basic Theory with Applications*, Butterworth-Heinemann: Oxford, **2000**; b) P. G. Vekilov, *Cryst. Growth Des.* **2010**, *10*, 5007–5019; c) J. Anwar, D. Zahn, *Angew. Chem. Int. Ed.* **2011**, *50*, 1996–2013; d) P. Yi, G. Rutledge, *Annu. Rev. Chem. Biomol. Eng.* **2012**, *3*, 157–182.
- R. Buller, M. Peterson, O. Almarsson, L. Leiserowitz *Cryst. Growth & Design*, **2002**, *2*, 553–562.
- D. Gebauer, A. Voelkel, H. Coelfen *Science*, **2008**, *322*, 1819 – 1822.
- P. Vekhilov, *Cryst. Growth & Design*, **2010**, *10*, 5007–5019.
- <https://www.statista.com/statistics/263102/pharmaceutical-market-worldwide-revenue-since-2001>
- I. Weissbuch, M. Lahav, L. Leiserowitz, *Cryst. Growth Des.* **2003**, *3*, 125–150.
- a) J. Chen, B. Trout, *J. Phys. Chem. B* **2008**, *112*, 7794–7802; b) D. Toroz, R. Hammond, K. Roberts, S. Harris, T. Ridley, *Cryst. Growth* **2014**, *401*, 38–43; c) M. Salvalaglio, C. Perego, F. Giberti, M. Mazzotti, M. Parrinello, *Proc. Natl. Acad. Sci. U.S.A.* **2015**, *112*, E6–E14; d) M. Salvalaglio, M. Mazzotti, M. Parrinello, *Faraday Discuss.* **2015**, *179*, 291–307.
- R. J. Davey, S. Schroeder, J. ter Horst, *Angew. Chem. Int. Ed.* **2013**, *52*, 2166–2179.
- a) R. Sullivan, R. J. Davey, G. Sadiq, G. Dent, K. Back, J. ter Horst, D. Toroz, R. Hammond, *Cryst. Growth Des.* **2014**, *14*, 2689–2696; b) R. Davey, K. Back, R. Sullivan, *Faraday Discuss.* **2015**, *179*, 9–26; c) J. Black, *Private Communication* **2017**.
- a) S. Jiang, J. H. ter Horst, *J. Cryst. Growth Des.* **2011**, *11*, 256–261; b) H. Yang, J. H. ter Horst in *New Perspectives on Mineral Nucleation and Growth*, (Eds A. E. S. van Driessche et al.), Springer International Switzerland, **2017**, pp 317–337.
- D. Rossi, A. Gavriilidis, S. Kuhn, M. Candel, A. Jones, C. Price, L. Mazzei, *Cryst. Growth Des.* **2015**, *15*, 1784–1791.
- a) D. Khamar, J. Zeglinski, D. Mealey, A. Rasmuson, *J. Am. Chem. Soc.* **2014**, *136*, 11664–11673; b) C. Brandel, J. ter Horst, *J. Faraday Discuss.* **2015**, *179*, 199–214; c) S. Kulkarni, S. Kadam, H. Meeke, A. Stankiewicz, J. ter Horst, *Cryst. Growth Des.* **2013**, *12*, 2435–2440; d) D. Mealey, J. Zeglinski, D. Khamar, A. Rasmuson, *Faraday Discuss.* **2015**, *179*, 309–328; e) H. Yang, A. Rasmuson, *Cryst. Growth Des.* **2015**, *13*, 4226–4238.
- We are only aware of one previous study for 3 alkyl parabens differing only in their alkyl chain lengths.^[8e]
- A total of 6186 crystallisation experiments were carried out – 2610 for BA, 930 for PTA, 1590 for PABA and 1056 for PNBA.
- Nucleation of PTA and PNBA from MeCN was so fast that measurements were not possible.
- C. Hansch, A. Leo, R. Taft, *Chem. Rev.* **1991**, *91*, 165–195.
- a) W. Du, A. J. Cruz-Cabeza, S. Woutersen, R. J. Davey, Q. Yin, *Chem. Sci.* **2015**, *6*, 3515–3524; b) C. Brooks, G. Eglinton, J. Morman, *J. Chem. Soc.* **1961**, 106–116; c) Y. Fujii, H. Yamada, M. Mizuta, *J. Phys. Chem.* **1988**, *92*, 6768–6772.
- FTIR bands indicative of acid dimers occur at identical positions for BA and PTA (1694 and 1695 cm⁻¹ in toluene; 1698 and 1700 cm⁻¹ in acetonitrile) while in acetonitrile the bands of weakly solvated monomers are again found at essentially identical positions 1725 and 1723 cm⁻¹.
- CNT equation fitting does not allow discrimination between interface and volume-diffusion control (ESI). We report here only the former values.
- Y. Xiao, S. K. Tang, H. Hao, R. J. Davey, T. Vetter, *Cryst. Growth Des.*, **2017**, *17*, 2852–2863.
- D. Coombes, R. Catlow, J. Gale, A. Rohl, S. L. Price, *Cryst. Growth Des.* **2005**, *5*, 879–885.
- S. Grimme, *J. Comput. Chem.* **2006**, *27*, 1787–1799.
- a) G. Kresse, J. Hafner, *J. Phys. Rev. B.* **1993**, *47*, 558–561; b) G. Kresse, J. Furthmüller, *J. Comput. Mater. Sci.* **1996**, *6*, 15–50; c) G. Kresse, J. Furthmüller, *J. Phys. Rev. B* **1996**, *54*, 11169–11186.
- K. Mathew, R. Sundararaman, K. Letchworth-Weaver, T. Arias, R. Hennig, *J. Chem. Phys.* **2014**, *140*, 084106 1–8.
- We justify the assumption of monomeric growth units on the basis of the solution chemistry - the formation of solution phase H-bonded dimers is not rate determining (see text and refs 8 and 9a). In doing this it follows that such dimers must form during molecular attachment to the cluster surface.
- A. Gavezotti, *Acta Cryst.* **2008**, *B64*, 401–403.
- E. Gaines, K. Maisuria, D. DiTommaso, *CrystEngComm*, **2016**, *18*, 2937–2948.
- M. J. Thomason, C. R. Seabourne, B. M. Sattelle, G. A. Hembury, J. S. Stevens, A. J. Scott, E. F. Aziz, S. L. M. Schroeder, *Faraday Discuss.* **2015**, *179*, 269–289.